

# A Poisson Kalman Filter to Control the Dynamics of Neonatal Sepsis and Postinfectious Hydrocephalus

Donald Ebeigbe<sup>\*1</sup>, Tyrus Berry<sup>\*2</sup>, Steven J. Schiff<sup>1,3,4</sup>, Timothy Sauer<sup>2</sup>

Neonatal sepsis (NS) and resulting complications, such as postinfectious hydrocephalus (PIH), are a significant cause of neonatal and infant mortality throughout the developing world. Addressing this problem requires dynamical modeling and estimation of the true state of the disease using realistic data collection schemes, followed by optimal allocation of resources to control the disease with a combination of prevention and treatment. To address these issues, we first develop a compartmental model for non-communicable infections, which are especially common with NS. Then, we develop a novel optimal linear filter for Poisson observations, characteristic of infectious diseases, which model the number of patients recorded as presenting each day at hospitals. The classical Linear Quadratic Regulator is generalized to nonautonomous linear dynamics with mixed linear and quadratic cost functions, which better model real world costs. At each step we apply our methods to a case study of NS and PIH, using parameters estimated from publicly available data for Uganda. We demonstrate the effectiveness of our filter in numerical experiments and study the effect of the economic cost of NS and PIH on the optimal allocation of resources between prevention and treatment. Our approach is applicable to a broad range of disease dynamics, and can be extended to the inherent nonlinearities of communicable infectious diseases.

PACS numbers:

\*Contributed equally.

<sup>1</sup>Center for Neural Engineering, Department of Engineering Science and Mechanics, The Pennsylvania State University, University Park, PA, USA

<sup>2</sup>Department of Mathematical Sciences, George Mason University, Fairfax, VA, USA

<sup>3</sup>Department of Neurosurgery, Penn State College of Medicine, Hershey, PA, USA

<sup>4</sup>Department of Physics, The Pennsylvania State University, University Park, PA, USA

## I. INTRODUCTION

Severe systemic bacterial infection in the neonatal period, neonatal sepsis (NS), accounts for an estimated 680,000 - 750,000 neonatal deaths per year worldwide [17] - more than childhood deaths from malaria and HIV combined [18]. The most common brain disorder in childhood is hydrocephalus, and the largest single cause of hydrocephalus in the world is as a sequelae of NS [8], accounting for an estimated 160,000 yearly cases of postinfectious hydrocephalus (PIH) in infancy [3]. The microbial agents responsible for this enormous loss of human life have been poorly characterized [14], although next-generation molecular methods show promise to improve the identification of causal agents [12]. Both NS and PIH occur disproportionately in the developing world, and most of the PIH cases will die in childhood without adequate treatment, substantially compounding the effective mortality due to NS and its tremendous burdens on societies [13, 22]. To our knowledge, there is no existing computational framework that embodies the interdependent dynamics of NS and PIH.

There has been significant recent interest in the model-based optimal control of contagious infectious disease, specifically using a prevention (in the form of vaccination) and treatment as methods of control [4, 19, 25–27]. Such model-based frameworks have been instrumental in our understanding of the dynamics and control of infectious diseases [7], and strategies for global public health policies [5]. These studies start from nonlinear compartmental models which are built on the standard SIR model and its variants. The SIR model tracks three variables which represent three populations, susceptible (S), infected (I), and recovered (R). A key feature is that the rate of increase of the infected is proportional to the product of the susceptible and infected populations,  $SI$ , a nonlinear interaction term that is motivated by the contagious nature of the diseases being modeled. However, balancing prevention and treatment is also critical in non-communicable diseases, especially when limited resources are available. In Section II below, we introduce an SIR model for non-communicable diseases. The lack of an interaction term renders this model completely linear.

Our goal is to draw from the available tools for state estimation and control, namely the Kalman filter [6] and the Linear Quadratic Regulator (LQR) [9]. These methods originated in an engineering context and make assumptions that may not be appropriate to the modeling, estimation, and control of disease. In particular, the Kalman filter assumes that at each time step one can make an observation that is directly proportional to the true number of infected up to a Gaussian perturbation. However, a more realistic model for patients presenting at a care center is a

Poisson random variable, especially when the expected rate of generation of infected patients is low. Even when the expected rate is high, and the Poisson distribution is well-approximated by a Gaussian, a Kalman filter assumes a fixed noise variance, whereas the variance of Poisson observations will change as the true number of infected changes. In Section IV we introduce the Poisson Kalman Filter (PKF) which adapts the Kalman filter to account for this type of observation.

In Section IV we argue that a Poisson random variable is a preferred model for disease occurrences, and then design an optimal linear filter for state estimation using this type of observation. For one-dimensional systems, an optimal filter has been previously designed for Poisson observations [11], but has not been generalized to multivariate systems. Moreover, in order to summarize the true distribution of the state  $\vec{x}_k$  at time step  $k$  given the Poisson observations in [11], a very large number of variables needed to be stored and recalculated at each step. In fact, the number of variables needed also grows very quickly with  $k$  (compared to the Kalman filter where the number of variables tracked is constant in  $k$ ). Instead, we propose a *linear* filter which is very similar to the Kalman filter, but is adapted to the unique statistics of the Poisson observations. A related linear filter called the Generalized Kalman Filter (GKF) was introduced in [28], which employed a fixed observation noise covariance matrix that is optimal among all linear filters that are fixed in time. In contrast, we will derive the optimal time-varying linear filter, and we will use the state estimate to update the observation noise covariance matrix dynamically.

Ensemble Kalman filters have seen recent use in infectious disease modeling [24] and are often used with nonlinear contagious dynamics while retaining a Gaussian noise assumption on the *a priori* and *a posteriori* error estimates. Although Kalman filters typically assume Gaussian distributed observations that have direct functional relationships to the state variables, this might not be suitable for diseases with low rates of occurrence – as is the case in the early stages of the spread of most infectious diseases. While a Poisson distribution with a large rate constant can be well approximated by a Gaussian of the same mean and variance, the approximation breaks down when the rates of occurrences are much smaller [2]. Even more importantly, the variance of a Poisson observation changes along with its mean, whereas the mean and variance of a Gaussian are decoupled, and often the variance is assumed to be constant (or at least unrelated to the mean) in the Kalman filtering context. In Section IV, we first show that by choosing an appropriate observation map, the standard Kalman filter gives an unbiased estimator for Poisson observations. This justifies using a Kalman filter in the disease modeling context, as long as the observation map is well chosen. We then show how to modify the Kalman equations to produce an optimal linear filter in the sense of minimizing the expected squared errors. While the optimal filter nominally requires knowledge of the true state, we show empirically that using the filter estimate of the state gives very similar performance. We call this approach the Poisson Kalman Filter (PKF).

Our ultimate goal in modeling and state estimation of disease is to control its prevalence. As in the case of the Kalman filter, we need to adapt the existing methods to the context of disease modeling. For example, the Linear-Quadratic Regulator (LQR) considers a purely linear model with a quadratic cost function. However, as we show in Section II, models for subsets of a population may require a forcing term. Moreover, in Section V we argue that designing realistic cost functions may require a mixture of linear and quadratic terms. In order to address these challenges, we generalize the LQR optimal control formulas to allow forcing and mixed linear and quadratic costs in Section V.

Nonlinear extensions of the Kalman filter and optimal control often follow standard strategies of generalizing the linear formulas (e.g. the Extended and Ensemble Kalman filters [15]). So while our developments are applied to linear models in this report, we expect that these developments will be the first step towards developing subsequent nonlinear extensions.

We start by introducing the linear compartmental model for non-communicable disease in Section II, which is applied to neonatal sepsis in Uganda using publicly available information in Section II A. We then extend the linear compartmental model to include PIH in infants in Section III. We then turn to motivating the Poisson model for observations in Section IV and we go on to develop the PKF, which is the optimal linear filter. In Section V we generalize the LQR optimal control system to allow for forced linear systems and mixed linear and quadratic costs, and we apply our method to controlling hydrocephalus under different cost trade-off assumptions. We discuss future directions both for more detailed study of NS and PIH, and for further extensions of the filtering and control methods in Section VI.

## II. AN SIR MODEL FOR NON-CONTAGIOUS DISEASE IN A RESTRICTED POPULATION

Consider a discrete-time SIR model for neonatal sepsis with three classes:  $S_k$  is the susceptible population at time  $k$ ,  $I_k$  the infected population, and  $R_k$  the recovered population. (Later, in Section III, the model will be expanded to include a postinfectious hydrocephalic class.) Since there are many unmodeled factors which affect the adult population, and the feedback of neonatal infection into the birth rate takes place on a relatively long time scale, we

do not include the adult population in the model. Thus,  $S_k, I_k, R_k$  represent neonatal and infant populations. Since we are modeling neonatal infections, the susceptible and infected classes are neonatal and,  $S_k + I_k$  represents the neonatal population. The recovered class,  $R_k$ , will track those that recover from sepsis for a period of time that can be chosen by the modeler as will be described below.

Modeling only the neonatal/infant populations requires several deviations from the standard SIR model. First, the birth rate is not proportional to any of the model populations, and is instead a forcing,  $b_k$ , which introduces new population into the susceptible class at each time step. Moreover, there are now three ways to leave the susceptible class: (1) a neonatal mortality rate  $d$ , due to factors other than infection (this will affect the two neonatal classes,  $S_k$  and  $I_k$ ), (2) an infection rate  $a$ , which feeds into the infected class, and (3) a ‘grow-up’ rate  $g_S$ , which signifies no longer being susceptible to neonatal infection. The model is:

$$S_{k+1} = (1 - d - a - g_S)S_k + b_k \quad (1)$$

$$I_{k+1} = (1 - d - d_I - c)I_k + aS_k \quad (2)$$

$$R_{k+1} = (1 - d_R - g_R)R_k + cI_k. \quad (3)$$

Notice that the  $g_S$  rate removes neonates from the model entirely, so effectively the grow-up rate  $g_S$  will control the length of time that we consider to be ‘neonatal’. Given a time period  $T_S$  for susceptibility, we set  $g_S = 1/T_S$ , which makes the simplifying assumption that the susceptible population is always equally distributed across different ages. The grow-up rate  $g_R$  controls the length of time that infants in the recovered class are tracked, so that  $g_R = 1/T_R$  where  $T_R$  is the amount of time we track the recovered class. The two parameters  $g_S, g_R$  control the two time scales for susceptibility and recovery (which will become more significant later when we consider the longer time-scale possibility of developing hydrocephalus), and  $c$  is the rate of recovery from infection.

With the state variable  $\vec{x}_k = (S_k, I_k, R_k)^\top$ , the matrix form of the evolution is

$$\vec{x}_{k+1} = F\vec{x}_k + \vec{b}_k$$

where

$$F = \begin{pmatrix} 1 - d - a - g_S & 0 & 0 \\ a & 1 - d - d_I - c & 0 \\ 0 & c & 1 - d - g_R \end{pmatrix} \quad \vec{b}_k = \begin{pmatrix} b_k \\ 0 \\ 0 \end{pmatrix}$$

If the birth rate is assumed to be constant  $b_k \equiv b$ , the steady state populations can be explicitly solved. Setting  $S_\infty \equiv S_{k+1} = S_k$  in susceptible population in (1) we can solve for  $S_\infty = \frac{b}{d+a+g_S}$ . Substituting this for  $S_\infty = S_k$  in (2) and setting  $I_\infty \equiv I_{k+1} = I_k$  in (2) we can solve for  $I_\infty$  and similarly we can solve for  $R_\infty$  giving steady state solution,

$$S_\infty = \frac{b}{d + a + g_S} \quad (4)$$

$$I_\infty = \frac{ab}{(d + d_I + c)(d + a + g_S)} \quad (5)$$

$$R_\infty = \frac{abc}{(d_R + g_R)(d + d_I + c)(d + a + g_S)} \quad (6)$$

These steady state solutions have important public health implications on the time scale where the birth rate is approximately constant. First,  $S_\infty$  determines the scale of public health improvement if susceptibility can be reduced (prevention). Second,  $I_\infty$  determines the resources needed to meet the average infection burden.

### A. Case Study: Neonatal sepsis in Uganda

Publicly available statistics can be used to approximate parameters for NS in Uganda during the time frame 2014-2015. We consider a discrete time step (the time between steps  $k$  and  $k + 1$ ) of one day and a neonatal period of  $T_S = 28$  days. From [21] we find a 2015 birth rate of 1665000 per year for Uganda, which for a daily model yields  $b \approx 4562$ . Using 2014 statistics for neonatal sepsis in sub-Saharan Africa, we find a neonatal mortality rate of 29 per 1000 with 17%-29% attributable to sepsis [13]. For simplicity we assume that the neonatal mortality rate of 29 per 1000 can be divided into 7 attributable to sepsis ( $\approx 23\%$  of neonatal mortality, the midpoint of the 17%-29% range) and 22 attributable to other causes.

Since we assume the neonatal period is  $T_S$  days, we convert the neonatal mortality rate due to factors other than sepsis into a daily rate by setting  $d = 22/1000/T_S$ . The daily neonatal mortality rate due to sepsis is then  $7/1000/T_S$ ,

- The neonatal time period,  $T_S$  (28 days)
- The infant time period,  $T_i$  (365 days)
- Daily birth rate,  $b$  (4562)
- Neonatal mortality rate,  $m_1$  (0.0029)
- Percentage of neonatal mortality due to sepsis,  $s$  (0.23)
- Infection rate,  $a$  (0.0030)
- Infant mortality rate,  $m_2$  (0.0077)

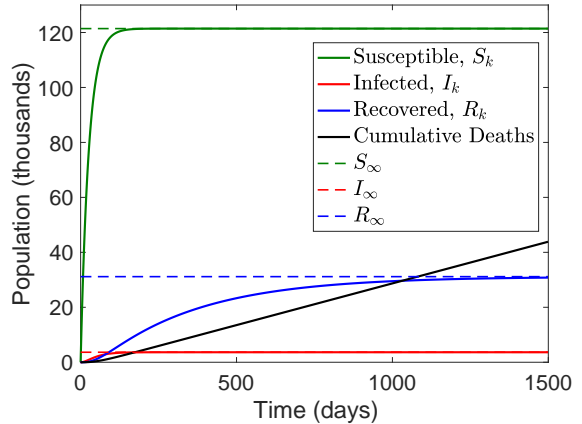


FIG. 1: Left: Summary of the inputs to the model for infant sepsis. Right: Simulation of the model for infant sepsis in Uganda assuming constant birth rate and starting from the zero initial condition,  $(S_0, I_0, R_0) = (0, 0, 0)$ .

however this is *not*  $d_I$  because the  $d_I$  variable applies only to the infected class (whereas  $d$  applies to both the susceptible and infected classes, and thus is a rate for the entire neonatal population). That is,  $d_I$  represents the daily rate of mortality due to sepsis as a percentage of the population that has sepsis (rather than  $7/1000/T_S$  which is the daily rate as a percentage of the entire population). So before we can determine  $d_I$ , we first must determine the infection rate  $a$ . Infection rate estimates can vary widely based on methodology ([13] quotes a range of 5.5 - 170 per 1000 live births). Based on the estimate of one of the authors (SJS) who is a physician conducting medical research on these infants in Uganda, there is a range of 30 - 60 per 1000 live births in that nation. Conservatively assuming 30 per 1000, we take  $a = 30/1000/T_S$  as a daily rate of infection. Now the constant  $d_I$  can be determined. We stated above that 7 of the 1000 will die from sepsis, meaning that 7 of the 30 who get sepsis will die from it. Thus, we find that  $d_I = 7/30/T_S$  is the daily rate of death due to sepsis among those that already have sepsis. This immediately gives us the recovery rate: 7 of the 30 who get sepsis will die from sepsis, and  $30(22/1000)$  will die from non-sepsis causes. The remaining  $30 - 7 - 30(22/1000) = 22.34$  will recover, establishing the recovery rate  $c = 22.34/30/T_S$ . Note that

$$c = \frac{30 - 7 - 30(22/1000)}{30T_S} = \frac{1}{T_S} - \frac{7}{30T_S} - \frac{22/1000}{T_S} = g_S - d_I - d$$

so in fact  $c$  is chosen to insure that all of the infected classes leave within the neonatal day period.

The infant mortality rate  $m_2$ , which covers mortality of the first year after birth, infancy or  $T_i$ , can also be derived from data. Consider a tracking time for the recovered population of this first year minus the neonatal period,  $T_R = T_i - T_S$  (we assume that the recovered population is entirely outside the 28 day neonatal period). For the death rate in the recovered class we start with the infant mortality rate of 77 per 1000 (in the first year [13]) and subtract the 29 per 1000 neonatal mortality rate to find  $d_R = 48/1000/T_R$ .

We summarize the inputs to the model in Fig. 1 then compute the parameters  $d, d_I, d_R, c, T_R, g_S, g_R$  by

$$\begin{aligned} g_S &= \frac{1}{T_S} & g_R &= \frac{1}{T_R} \\ d &= \frac{(1-s)m_1}{T_S} & d_I &= \frac{sm_1}{aT_S} \\ c &= g_S - d - d_I & d_R &= \frac{m_2 - m_1}{T_R} \end{aligned}$$

where  $s$  is the fraction of neonatal mortality due to sepsis. The steady state values for the model with these parameters are  $S_\infty = 121422$ ,  $I_\infty = 3643$ , and  $R_\infty = 31152$ . We note that the steady state number of infected shows consistency with reported values [21]. The recovered class is now susceptible to developing PIH.

### III. SIRH: MODELING THE HYDROCEPHALIC POPULATION

We now turn to a model that specifically links neonatal infection and postinfectious hydrocephalus (PIH). The essential idea is that those that have recovered from sepsis are now susceptible to developing hydrocephalus. The

constant  $h$  represents the rate at which recovered infants move from the recovered class  $R_k$  to a new hydrocephalic class  $H_k$ , leading to the equations

$$\begin{aligned} S_{k+1} &= (1 - d - a - g_S)S_k + b_k \\ I_{k+1} &= (1 - d - d_I - c)I_k + aS_k \\ R_{k+1} &= (1 - d_R - g_R - h)R_k + cI_k \\ H_{k+1} &= (1 - d_R - d_H)H_k + hR_k. \end{aligned} \tag{7}$$

The hydrocephalic class is subject to an additional mortality rate due to hydrocephalus,  $d_H$ , which requires recalibrating the recovered rate,  $d_R$ , so that it does not include deaths due to hydrocephalus. We set  $d_R = (m_2 - m_1 - p d_H T_R) / T_R$  where  $m_2$  is the infant mortality rate,  $m_1$  is the neonatal mortality rate,  $p$  is the rate of PIH in the total population under consideration (discussed in Section III A below), and  $d_H T_R$  is the rate of death of those who develop PIH during infancy ( $d_H$  is the daily rate and  $T_R$  is the remainder of the infancy period). Finally, we note that the steady state value of the recovered class changes from the SIR model due to the rate  $h$ , and the new steady state along with the hydrocephalic steady state are given by

$$R_\infty = \frac{abc}{(d_R + g_R + h)(d + d_I + c)(d + a + g_S)} \tag{8}$$

$$H_\infty = \frac{hR_\infty}{d_R + d_H} = \frac{abch}{(d_R + g_R + h)(d + d_I + c)(d + a + g_S)(d_R + d_H)} \tag{9}$$

We now return to our case study of modeling PIH in Uganda.

#### A. Case Study: Infant hydrocephalus in Uganda

The first parameter to consider is  $h$ , the rate of developing postinfectious hydrocephalus (PIH). In [13] it is reported that the incidence of PIH is 3-5 per 1000 live births. We will take the low estimate of 3 per 1000 setting  $p = 3/1000$ , since it will be shown to be more consistent with other statistics below. Recall that above we estimated that for 1000 live births there are 30 cases of sepsis, and 22.34 of those recover. Since only recovered sepsis cases can develop PIH, this implies a rate of developing hydrocephalus of

$$h = 3/22.34/T_R.$$

The death rate due to hydrocephalus is highly dependent upon treatment. The untreated death rate is estimated at 50%, while treatment can reduce this to 25%. We will return to this distinction when we consider the control problem, for now we assume an overall death rate of 33% [23] and we set

$$d_H = 1/3/T_R.$$

Finally, we recalibrate the death rate for those recovering from sepsis by removing the deaths due to hydrocephalus (since those are accounted for in the  $H_k$  variable). So we set

$$d_R = \frac{m_2 - m_1 - p d_H T_R}{T_R} = \frac{.0077 - .0029 - .0003\frac{1}{3}}{T_R} = \frac{.0047}{T_R}$$

The results shown in Fig. 2 predict a steady state of approximately 10000 ongoing cases of PIH with an annual PIH incidence of approximately 4000 per year ( $365 * h * R_\infty$ ), and annual deaths due to PIH of approximately 3300, consistent with existing estimates [22].

#### IV. DATA ASSIMILATION FROM POISSON OBSERVATIONS

Estimating the current state (e.g.  $S_k, I_k, R_k$ , and  $H_k$ ) of the system is a critical challenge when applying compartmental modeling to disease forecasting and control. Data assimilation is a method of estimating the state from a time series of noisy observations. In particular, for linear systems such as (7), the Kalman filter [6] gives the optimal state estimate (minimal variance) and also quantifies the uncertainty in the estimate. However, the Kalman filter was designed for engineering applications where the observations are assumed to have a direct functional relationship to the state variables, except perturbed by Gaussian noise.

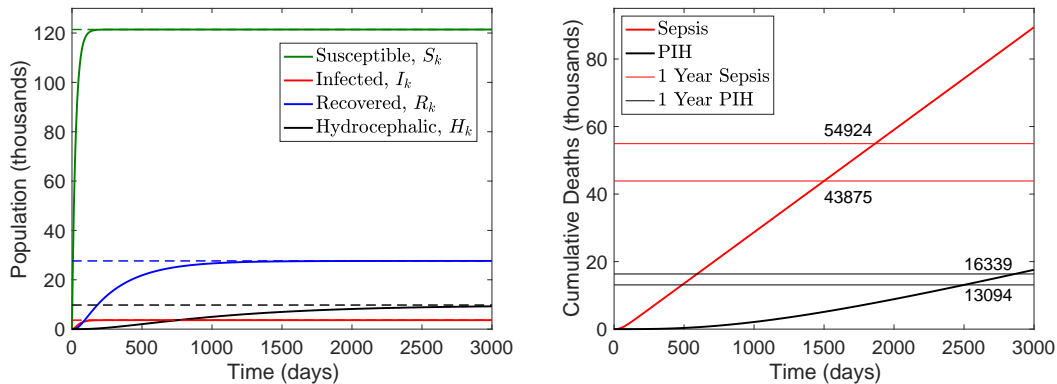


FIG. 2: Left: Simulation of the SIRH model for Uganda starting from the zero initial condition. Right: Plot of the cumulative deaths from sepsis and hydrocephalus in the simulation. The horizontal lines are spaced so that their intersections with the curves are 365 days apart and indicated the cumulative deaths at times one year apart. The model predicts approximately 11000 annual deaths due to sepsis and approximately 3300 annual deaths due to PIH.

There are at least three reasons why this assumption fails for typical disease surveillance. First, counts of individuals with a disease are by definition nonnegative, contradicting the Gaussian model for uncertainty. Second, the size of the Gaussian noise is decoupled from the population count, being the same magnitude for low populations as for large populations. Finally, in order for the population to be the observed variable, one would have to make a survey, at each time step  $k$ , of the entire population to directly observe (for example),  $H_k$ , the number of infants that have hydrocephalus at time  $k$ . Since this is an unrealistic proposal, the filtering method needs to be adapted to the type of observations that are practical for disease surveillance. We will refer to this modification of the Kalman filter by the name Poisson Kalman Filter (PKF), which we show to be unbiased and optimal among all linear filters.

We operate under that assumption that the disease population cannot be measured directly. In fact, a reasonable model for observations of disease cases, for example those presenting at a hospital, is a Poisson process, whose rate is proportional to the infected population. For example, at any given time step  $k$ , the number of new hydrocephalus patients will be approximated by a Poisson random variable with rate  $\lambda_{k,H} = c_H H_k$ , where  $c_H$  is the proportionality constant. Similarly, the number of new cases of infant sepsis will be approximated by a Poisson random variable with rate  $\lambda_{k,I} = c_I I_k$ . In the filtering context we map the state vector  $\vec{x} = (S_k, I_k, R_k, H_k)^\top$  to the observation with a matrix  $B$ , so in this case we can write,

$$\begin{pmatrix} \lambda_{k,I} \\ \lambda_{k,H} \end{pmatrix} = Bx_k = \begin{pmatrix} 0 & c_I & 0 & 0 \\ 0 & 0 & 0 & c_H \end{pmatrix} \begin{pmatrix} S_k \\ I_k \\ R_k \\ H_k \end{pmatrix}.$$

In a typical filtering problem we would assume that we are given direct observations,  $\vec{y}_k$ , of the form  $B\vec{x}_k + \vec{v}_k$  where  $\vec{v}_k$  are random variables representing observation noise. However, in the Poisson observation context, we instead observe a pair of independent Poisson random variables with rates given by the components of  $B\vec{x}_k$ . We will denote this type of observation by

$$\vec{y}_k \sim \text{Poisson}(B\vec{x}_k)$$

meaning that  $(\vec{y}_k)_i$  is Poisson with rate  $(B\vec{x}_k)_i$ . To be more precise we assume that, conditional to  $B\vec{x}_k$ , the components  $(\vec{y}_k)_i$  are independent Poisson random variables with density function,

$$P((\vec{y}_k)_i = z | (B\vec{x}_k)_i = \lambda) = \frac{\lambda^z}{z!} e^{-\lambda} = \frac{((B\vec{x}_k)_i)^{(\vec{y}_k)_i}}{((\vec{y}_k)_i)!} e^{-(B\vec{x}_k)_i}.$$

The above conditional density makes it clear that  $\vec{y}_k$  and  $\vec{x}_k$  are not independent.

In the case of direct observations, one typically assumes that  $\vec{y}_k$  splits into a sum of two terms, the first of which has deterministic dependence on  $\vec{x}_k$  and the second of which is independent of  $\vec{x}_k$ . However, for Poisson observations this splitting is not possible. Despite this irreconcilable dependence between  $\vec{y}$  and  $\vec{x}$  the following Lemma shows that if we appropriately center  $\vec{y}$ , namely  $\vec{y} - \mathbb{E}[\vec{y} | \vec{x}]$ , the result is not correlated with  $\vec{x}$ .

**Lemma IV.1.** *Let  $\lambda$  be an arbitrary random variable and let  $z$  be a Poisson random variable with rate  $\lambda$  so that the conditional density of  $z$  is  $P(z | \lambda) = \frac{\lambda^z}{z!} e^{-\lambda}$ . Then  $\mathbb{E}[(\lambda - \mathbb{E}[\lambda])(z - \mathbb{E}[z | \lambda])] = 0$ .*

*Proof.* We first apply the law of total expectation to compute  $\mathbb{E}[z] = \mathbb{E}[\mathbb{E}[z | \lambda]] = \mathbb{E}[\lambda]$  since  $\lambda$  is the expected value of a Poisson random variable with known rate  $\lambda$ . We then apply the law of total expectation,

$$\begin{aligned} \mathbb{E}[(\lambda - \mathbb{E}[\lambda])(z - \mathbb{E}[z | \lambda])] &= \mathbb{E}[\mathbb{E}[(\lambda - \mathbb{E}[\lambda])(z - \mathbb{E}[z | \lambda]) | \lambda]] \\ &= \mathbb{E}[(\lambda - \mathbb{E}[\lambda])\mathbb{E}[(z - \mathbb{E}[z | \lambda]) | \lambda]] \\ &= \mathbb{E}[(\lambda - \mathbb{E}[\lambda])(\mathbb{E}[z | \lambda] - \mathbb{E}[z | \lambda])] = 0 \end{aligned}$$

where the second equality follows from the inner expectation being conditioned on  $\lambda$  and the third follows from the linearity of the expectation.  $\square$

Lemma IV.1 turns out to be the key to deriving an optimal linear filter for Poisson observations. While Poisson observations are a more realistic model for the type of data available in disease modeling, we now must design a filter which can assimilate this data and produce estimates of the state variable  $\vec{x}_k$ .

### A. The Poisson Kalman Filter (PKF)

A linear filter produces an estimate  $\hat{x}_k$  of the true state  $\vec{x}_k$  of the form,

$$\hat{x}_k = W_1 \hat{x}_{k-1} + W_2 \vec{y}_k$$

where  $W_1, W_2$  are matrices. This is a more restricted class of filters, but we will be able to show that our filter is unbiased, meaning  $\mathbb{E}[\hat{x}_k] = \vec{x}_k$ , and is the optimal linear filter in the sense of giving the minimal squared error.

The PKF assumes a model of the form,

$$\vec{x}_k = F\vec{x}_{k-1} + \vec{b}_k + \vec{\omega}_{k-1} \quad (10)$$

$$\vec{y}_k \sim \text{Poisson}(B\vec{x}_k) \quad (11)$$

where  $\vec{b}_k$  is a known deterministic forcing term, and  $\vec{\omega}_k$  is dynamical noise with mean zero ( $\mathbb{E}[\vec{\omega}_k] = 0$ ) and known covariance matrix,  $\mathbb{E}[\vec{\omega}_k \vec{\omega}_k^\top] = W$ . We also assume that the  $\vec{\omega}_k$  are independent of  $\vec{x}_k, \vec{y}_k$ , and all other  $\vec{\omega}_\ell$  for  $\ell \neq k$ . The PKF also assumes that model,  $F$ , and observation matrices,  $B$ , are known. We note that the dynamics  $F$  and observation matrix  $B$  can also be allowed to change at each step (non-autonomous), but to simplify the notation we assume they are constant.

Like the standard Kalman filter, the PKF is a two-step filter, meaning that it breaks down the estimation of  $\hat{x}_k^+$  from  $\hat{x}_{k-1}^+$  into a forecast step and an assimilation step. In the forecast step we apply the model to our current estimate  $\hat{x}_{k-1}^+$  to produce the forecast,

$$\hat{x}_k^- = F\hat{x}_{k-1}^+ \quad (12)$$

and in the assimilation step we *assimilate* the new observation by,

$$\hat{x}_k^+ = \hat{x}_k^- + K_k(y_k - B\hat{x}_k^-). \quad (13)$$

It is easy to see that this is a linear filter with  $W_1 = (I - K_k B)F$  and  $W_2 = K_k$ . The filter is defined by the choice of the matrix  $K_k$  which is called the *gain matrix*. Our first result is that any filter of the form (13) is unbiased.

**Theorem IV.2.** *Assume that  $\mathbb{E}[\hat{x}_0] = \vec{x}_0$ , then for any choice of gain matrices  $K_k$  the two step filter defined by (12) and (13) is unbiased, meaning  $\mathbb{E}[\hat{x}_k] = \vec{x}_k$ .*

The proof of Theorem IV.2 is straightforward and can be found in A.1. The gain matrix is determined by a secondary set of computations which track the covariance matrix,  $P_k^+$  for the estimate  $\hat{x}_k^+$ . The covariance matrix is also evolved according to a two step evolution starting with a forecast step,

$$P_k^- = FP_{k-1}^+ F^\top + W$$

which allows us to calculate the optimal gain matrix,

$$K_k = P_k^- B^\top (BP_k^- B^\top + V_k)^{-1} \quad (14)$$

and then we can complete the assimilation step

$$P_k^+ = (I - K_k B) P_k^- (I - K_k B)^\top + K_k V_k K_k^\top.$$

While it may seem that  $P_k$  is only really necessary in order to compute the gain matrix  $K_k$ , the matrix  $P_k$  also gives an error estimate for the state estimate.

The final component that is required is the  $V_k$  matrix in the formula for the optimal gain. In the standard Kalman filter,  $V_k$  is the covariance matrix for the observation noise. However, in the PKF the variance of the observations is equal to  $B\bar{x}_k$  (meaning  $\text{var}((\bar{y}_k)_i) = (B\bar{x}_k)_i$ ). So intuitively, we would expect to use  $V_k = \text{diag}(B\bar{x}_k)$ . The next theorem states that this yields the optimal linear filter.

**Theorem IV.3.** *Among all linear filters, the filter given by (12) and (13) with gain matrix  $K_k$  given by (14) where  $V_k = \text{diag}(Bx_k)$  is optimal in the sense of minimal sum of squared errors. In other words,*

$$\frac{\partial J_k}{\partial K_k} = 0$$

where

$$J_k = \text{trace}(P_k) = \mathbb{E}[\|\hat{x}_k - \bar{x}_k\|_2^2] = \sum_i \mathbb{E}[(\hat{x}_k - \bar{x}_k)_i^2]$$

The proof of Theorem IV.3 is closely related to Lemma IV.1 and can be found in A.2. Unfortunately, the optimal filter is not accessible since it requires access to the true state  $\bar{x}_k$  in order to define the optimal gain matrix. Instead, since  $\hat{x}_k$  is an unbiased estimator (for any gain matrix) we approximate the optimal filter by using  $V_k = B\hat{x}_k^-$ . We call this approximation the Poisson Kalman Filter (PKF).

The discrete-time Poisson Kalman filter (PKF) algorithm is given below. In order to connect with the next section, we include the control term  $G_{k-1}\bar{u}_{k-1}$ . If there is no control this term can be dropped. We also allow all the matrices to vary with time.

#### 1 Dynamical system

$$\begin{aligned} \bar{x}_k &= \max(0, F_{k-1}\bar{x}_{k-1} + G_{k-1}\bar{u}_{k-1} + \bar{b}_k + \bar{w}_{k-1}), & \bar{w}_k &\sim \mathcal{N}(0, W_k) \\ \bar{y}_k &\sim \text{Poisson}(B_k\bar{x}_k) \\ \mathbb{E}[\bar{w}_k \bar{w}_j^\top] &= W_k \delta_{k-j} \\ \mathbb{E}[\bar{y}_k \bar{y}_j^\top] &= \text{diag}(B_k\bar{x}_k) \delta_{k-j} \\ \mathbb{E}[w_k y_j^\top] &= 0 \end{aligned} \tag{15}$$

where  $\delta_{k-j}$  is the Kronecker delta function, such that  $\delta_{k-j} = 1$  if  $k = j$ , and  $\delta_{k-j} = 0$  if  $k \neq j$ . When the state is close to zero the Gaussian noise may move the system into negative values, so at each step we take the maximum of each component and zero. Note that  $\text{diag}(B_k\bar{x}_k)$  is the true variance of the Poisson observation  $\bar{y}_k$ . However, in the filter below we set  $V_k = \text{diag}(B_k\hat{x}_k^-)$  since this is the best available estimate. We now summarize the steps required to obtain the PKF estimates.

#### 2 Initialization

$$\begin{aligned} \hat{x}_0^+ &= \mathbb{E}[\bar{x}_0] \\ P_0^+ &= \mathbb{E}[(\bar{x}_0 - \hat{x}_0^+)(\bar{x}_0 - \hat{x}_0^+)^\top] \end{aligned} \tag{16}$$

#### 3 Prior estimation (forecast step)

$$\hat{x}_k^- = F_{k-1}\hat{x}_{k-1}^+ + G_{k-1}\bar{u}_{k-1} + \bar{b}_k \tag{17}$$

$$P_k^- = F_{k-1}P_{k-1}^+ F_{k-1}^\top + W_{k-1} \tag{18}$$

$$V_k = \text{diag}(\max(\delta, B_k\hat{x}_k^-)) \tag{19}$$

#### 4 Posterior estimation (assimilation step)

$$K_k = P_k^- B_k^\top (B_k P_k^- B_k^\top + V_k)^{-1} \tag{20}$$

$$\hat{x}_k^+ = \max(0, \hat{x}_k^- + K_k (\bar{y}_k - B_k \hat{x}_k^-)) \tag{21}$$

$$P_k^+ = (I - K_k B_k) P_k^- (I - K_k B_k)^\top + K_k V_k K_k^\top \tag{22}$$

Notice that before the diagonal matrix  $V_k$  is formed, we first take the maximum of the diagonal entries and a constant  $\delta$ . This is necessary because when the diagonal entries of  $V_k$  are too close to zero the filter can become numerically unstable. The constant  $\delta$  should be chosen to be small relative to the average value of the  $B_k \bar{x}_k$ , and in all our numerical experiments we set  $\delta = 0.1$ . Finally, we note that in practice the initial estimates  $\bar{x}_0^+$  and  $P_0^+$  are often not available. However, the effect of these initial estimates on the accuracy of the state estimates decays to zero exponentially as  $k \rightarrow \infty$ , and often  $P_0^+$  is simply chosen to be a multiple of the identity matrix.

## B. PKF Simulations

Using the SIRH model described in Section III, we evaluate the performance of the PKF when the observations follow a random Poisson distribution with known rates  $\lambda_{k,I} = c_I I_k$  and  $\lambda_{k,H} = c_H H_k$ , which represent the number of infants with sepsis and the number of infants with hydrocephalus that show up at the hospital. Our observations can be written as

$$y_k = \begin{pmatrix} y_{k,1} \\ y_{k,2} \end{pmatrix} = \text{Poisson} \begin{pmatrix} \lambda_{k,I} \\ \lambda_{k,H} \end{pmatrix}, \quad \text{where} \quad \begin{pmatrix} \lambda_{k,I} \\ \lambda_{k,H} \end{pmatrix} = Bx_k = \begin{pmatrix} 0 & c_I & 0 & 0 \\ 0 & 0 & 0 & c_H \end{pmatrix} \begin{pmatrix} S_k \\ I_k \\ R_k \\ H_k \end{pmatrix}.$$

and we start the system at the equilibrium values.

The simulation in Fig. 3 was run with system noise  $W = \text{diag}(144, 1, 1, 10) \times 10^7$  and the constant daily birth rate  $b = 4562$ , while setting the sepsis and hydrocephalus proportionality constants as  $c_I = 0.2/T_S$  and  $c_H = 0.6/T_R$  respectively. The idea behind these values is that if 20% of total sepsis cases seek care over the entire  $T_S$  period of sepsis susceptibility, then the daily rate of arrivals would be  $0.2/T_S$  multiplied by the number of true sepsis case (20% was chosen purely for purposes of simulation). In Fig. 3 we see that the PKF (red, dashed curves) gave good estimates of the true susceptible, infected, recovered, and hydrocephalic populations using only random Poisson distributed observations of the sepsis and hydrocephalic populations.

Fig. 3 also compares the PKF to a Kalman filter (blue, dotted curves) which was given the optimal fixed observation noise covariance matrix,  $V_{\text{const}} = \text{diag}(B\bar{x})$  where  $\bar{x}$  is the time average of the state variables. The disadvantage of the fixed gain is that when the number of infected or hydrocephalic is large the variance of the observations will be larger than the average value. This means that the Kalman filter will underestimate the observation variance and use an oversized gain. This is shown in Fig. 3 where the Kalman filter estimates closely follows the observations when the number of infected or hydrocephalic are large. The PKF dynamically adjusts the observation covariance matrix based on the state estimate in order to prevent this. This is further shown in Fig. 5 which compares the RMSE for the PKF and the Kalman filter for various levels of system noise. Fig. 5 also compares the PKF, which uses the filter estimate to determine  $V_k$ , to an oracle PKF which uses the true state for  $V_k$  and we see that their performance is almost identical even at high noise levels.

Finally, we note that the PKF has the largest advantage at high noise levels. This is because the SIRH system is a stable linear system, so that noise is the only unstable component of the dynamics. In the absence of noise, no filter would be necessary since all trajectories would converge to the equilibrium regardless of observations. This suggests that a generalized PKF (such as an extended or ensemble version of the PKF) would have an advantage for nonlinear dynamics with unstable directions even in the absence of system noise.

## V. OPTIMAL CONTROL FOR LINEAR COMPARTMENTAL MODELS

The goal of optimal control is to augment the dynamics of the model with a *control variable*  $u_k$ , which is assumed to have a known effect on the state given by (in the linear context),

$$\vec{x}_{k+1} = F\vec{x}_k + G\vec{u}_k + \vec{b}_k \quad (23)$$

where  $\vec{b}_k$  is a known deterministic forcing term. The control  $\vec{u}_k$  may have some constraints, and also has an associated cost functional,  $J(x, u)$ , which determines the cost of the both the control and the state as well as the tradeoff between them. The goal of optimal control is to choose the control  $u$  which minimizes the cost, so clearly the choice of  $J$  is fundamental and implicitly determines our priorities. For example, below we will consider prevention and treatment as controls that compete for resources, so the  $J$  functional will need to contain the cost of prevention and treatment as well as the cost of the state which includes the number of septic and hydrocephalic infants. Control strategies for prevention (vaccination) and treatment have been considered extensively for nonlinear SIR models for contagious

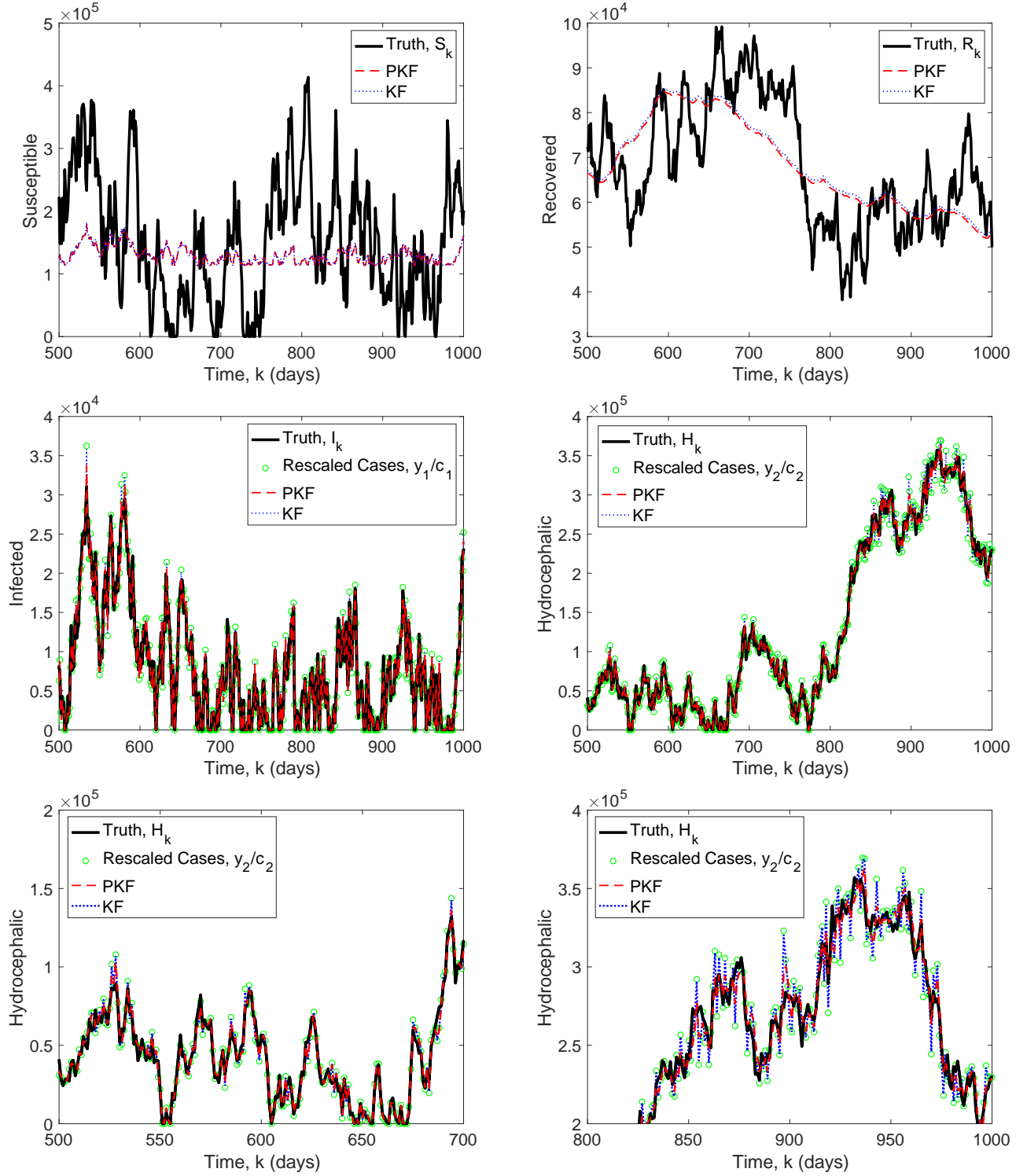


FIG. 3: Comparison of the PKF (optimal variable gain) and the Kalman filter (optimal fixed gain) for the SIRH model with Poisson observations of the infected and hydrocephalic populations. The top and middle panels compare the true  $S$ ,  $I$ ,  $R$  and  $H$  values (black) to the PKF (red, dashed) and Kalman filter (blue, dotted) estimates. Infected and hydrocephalic also show the observations (green, circles) rescaled by dividing by the constants  $c_1$ ,  $c_2$  respectively. The bottom row of panels are expanded versions of the  $H$  plot in middle right panel, enlarged to show detail. When the number of cases is large, the KF estimate of  $H$  is very close to the observations, whereas the PKF adjusts to the larger observation variance and produces better estimates.

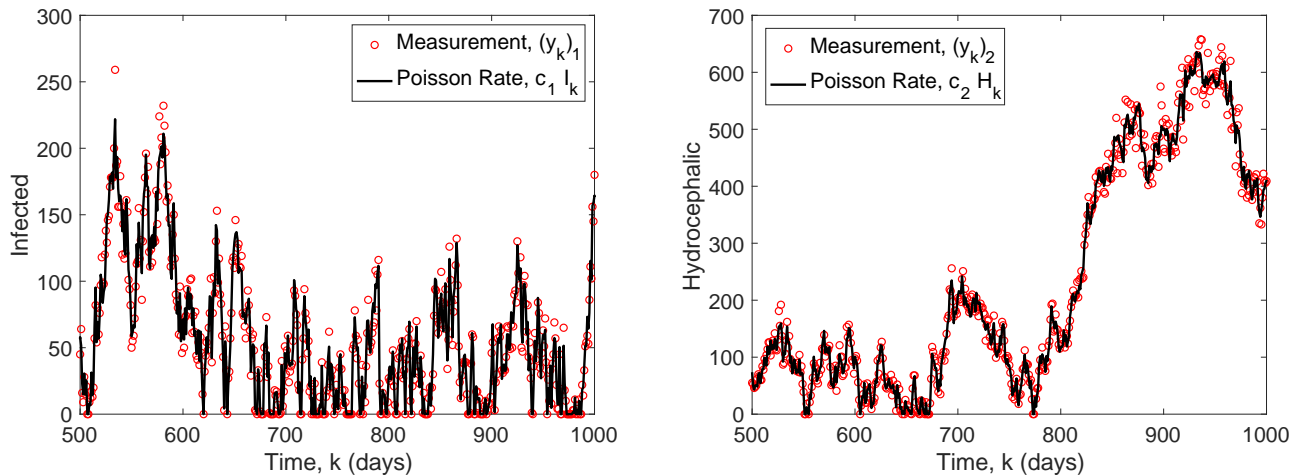


FIG. 4: The Poisson rates (black) of I and H and the observed case numbers (red, circles) from the Poisson distribution.

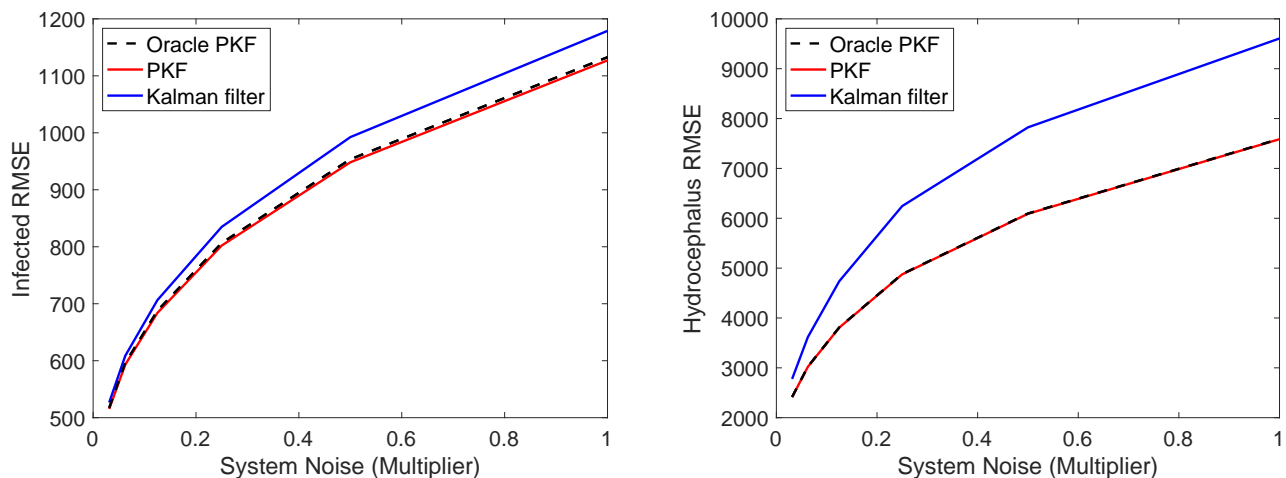


FIG. 5: Comparison of the RMSE of the PKF (red, optimal variable gain) and the Kalman filter (blue, optimal fixed gain) as function of the system noise. We also compare to an oracle PKF (black, dashed) which is given the optimal choice of  $V_k = \text{diag}(B\bar{x}_k)$ . System noise is quantified as a multiple of the base noise level  $W$ . The RMSE is averaged over  $10^6$  filter steps,

disease [4, 19, 25–27]. In our context we consider non-contagious disease which leads to a linear model. This means that explicit solutions for optimal control are possible (unlike the nonlinear setting). However, the classical results for linear models do not include forcing and have purely quadratic costs. As shown in Section II, our model requires forcing in order to account for births, and below we will motivate the need for mixed quadratic and linear costs. We then present a new explicit solution for the optimal control in this extended context (including forcing and mixed quadratic and linear costs). We now consider some standard forms for the cost function and consider their advantages and disadvantages before presenting our compromise between these choices.

### A. Quadratic and linear costs

One of the most common cost functionals is the quadratic cost,

$$J(x, u) = \bar{x}_T^\top Q_f \bar{x}_T + \sum_{k=1}^T \bar{x}_k^\top Q \bar{x}_k + \bar{u}_k^\top R \bar{u}_k \quad (24)$$

where  $Q_f$  defines the cost of the final state  $\vec{x}_T$ , and  $Q, R$  define the cost of the state and control respectively. Both  $Q_f$  and  $Q$  are assumed to be non-negative definite and  $R$  is assumed to be positive definite. Notice that the relative scale of  $Q$  and  $R$  implicitly defines a tradeoff between the control and the state. If we take the infinite time horizon problem  $T = \infty$  then we drop the  $Q_f$  term. The quadratic cost functional (24) defines a convex optimization problem and has an explicit solution in the form of the Linear Quadratic (LQ) controller for (23). We should note that the classical solutions do not include the forcing term  $\vec{b}_k$  which is included in the generalized result below.

In addition to the advantage of having an explicit optimal solution, the quadratic cost functional is also often motivated by the idea that marginal costs may grow as one tries to increase the control, leading to greater than proportional costs. For example, when we consider prevention and treatment as controls, if we attempt to reach larger and larger portions of society they may be further from population centers and require higher marginal costs. On the other hand, there may be economies of scale that actually reduce marginal costs at some levels, and costs may even be close to proportional over some range of the controls. Moreover, especially when we consider the cost associated with the state, the quadratic cost has other potential disadvantages.

For example, with the SIRH model, consider a  $Q$  matrix that is all zeros except for the (4,4)-entry, which yields a cost proportional to  $\sum_{k=1}^T H_k^2$ . A potential issue is that minimizing this sum does not minimize the total number of hydrocephalus cases which would be  $H_T = \sum_{k=1}^T H_k$ . For example, if  $H_T$  are equally distributed in time, the quadratic cost is  $H_T^2/T$  whereas if all  $H_T$  occur at the final time  $k = T$  the cost would be much larger  $H_T^2$ . This would imply that it is preferable to have  $\sqrt{T}H_T$  cases evenly spread across  $T$  time steps as opposed to  $H_T$  at one time. Of course, in terms of ability to treat cases there may be valid reasons to prefer equidistribution of cases in time, especially if hospital capacity to manage the cases would be exceeded.

Therefore the goal of minimizing the number of hydrocephalus cases may suggest using a linear cost functional

$$J(x, u) = \sum_{k=1}^T \vec{x}_k^\top \vec{q} + \vec{u}_k^\top \vec{r} \quad (25)$$

where  $\vec{q}, \vec{r}$  are vectors that determine the relative costs of the state and controls. However, this choice leads to the opposite problems of the quadratic functional. The linear cost does not capture potential increases of marginal costs for large controls, potentially leading to unrealistic strategies, and the linear cost does not penalize unequal distribution of cost which could overwhelm available resources. Even more problematic is that the linear cost does not define a strictly convex optimization problem and so there will typically be no optimal solution but instead the system may try to send control variables to infinity to obtain unlimited ‘negative’ costs. This can be overcome by constraining the controls in which case the optimal control is typically obtained on the boundary of the feasible control space.

The foregoing discussion suggests a compromise between the quadratic and linear cost functionals. Thus we consider the cost functional

$$J(x, u) = \vec{x}_T^\top Q_f \vec{x}_T + \vec{x}_T^\top \vec{q}_f + \sum_{k=1}^T \frac{1}{2} \vec{x}_k^\top Q \vec{x}_k + \vec{x}_k^\top \vec{q} + \frac{1}{2} \vec{u}_k^\top R \vec{u}_k + \vec{u}_k^\top \vec{r}$$

which mixes the linear and quadratic costs. In B we show that the optimal control is given by

$$\vec{u}_k = -(R + G^\top P_{k+1} G)^{-1} (G^\top (P_{k+1} (F \vec{x}_k + \vec{b}_k) + \vec{p}_{k+1}) + \vec{r}) \quad (26)$$

where  $P_k$  is given by the discrete Riccati equation

$$P_k = F^\top P_{k+1} F - F^\top P_{k+1} G (R + G^\top P_{k+1} G)^{-1} G^\top P_{k+1} F + Q$$

and  $\vec{p}_k$  is given by

$$\vec{p}_k = F^\top (P_{k+1} \vec{b}_k + \vec{p}_{k+1}) - F^\top P_{k+1} G (R + G^\top P_{k+1} G)^{-1} (G^\top (P_{k+1} \vec{b}_k + \vec{p}_{k+1}) + \vec{r}) + \vec{q}.$$

Both  $P_k$  and  $\vec{p}_k$  are solved for by starting from  $k = T$  and iterating backwards in time starting from  $P_T = Q_f$  and  $\vec{p}_T = \vec{q}_f$ . Note that when  $\vec{q}, \vec{q}_f, \vec{r}$ , and  $\vec{b}_k$  are all zero we find  $p_k = 0$  and the optimal control reduces to the classical linear quadratic regulator. In B we also give the steady state solution for the infinite time horizon problem (where  $T = \infty$ ,  $q_f = 0$ , and  $Q_f = 0$ ).

## B. Case study: SIRH control via prevention and treatment

The model (7) is sufficient for tracking hydrocephalus, but a key motivation for modeling is to study different control strategies. We will consider two methods of controlling hydrocephalus, prevention and treatment. Prevention (in a form such as vaccination) and treatment are considered extensively in the literature for nonlinear models for contagious disease [4, 19, 25–27]. In the nonlinear context, it is advantageous to consider a proportional control, for example, the control variable for prevention is constrained to be in  $[0, 1]$  and represents the proportion of susceptibles that are treated at each time step. However, this means the control variable must be multiplied by the state variable  $S_k$ , which is a nonlinear interaction between the control and the state. For nonlinear models such as those considered in [4, 19, 25–27] this is not a disadvantage since the systems are already nonlinear, however in our case we would like to preserve the linearity of the model. Thus, rather than proportional control, our control variables will be the number of susceptibles to whom prevention is applied. The only disadvantage of this approach is that rather than being constrained to  $[0, 1]$  the prevention is now constrained to  $[0, (1 - d - a - g_S)S_k + b_k]$  which prevents  $S_{k+1}$  from becoming negative (see equation (27) below). This time varying constraint is simple to implement as we will describe below.

In our model, prevention is applied to those in the susceptible class and directly reduces the number of susceptibles by  $P_k$ . The number  $P_k$  is consider the number of *effective* preventions, so this number of susceptibles are now considered safe from infection and are removed from the model entirely. However, we do not assume that the prevention strategy is 100% effective, instead we assume that the cost function is accounting for the total cost to reach  $P_k$  effective preventions (which implicitly may include the cost of larger number of total preventions). Similarly, we let  $T_k$  be the number of effective treatments, incorporating the cost of ineffective treatments implicitly in the cost functional. Treatment is applied to the infected class, and moves them into a new recovered class which will have different characteristics than those that recover without treatment. This necessitates the creation of two distinct recovered classes, those that recovered due to treatment,  $R_k^t$ , and those that recovered despite being untreated,  $R_k^u$ . This leads to the following system of equations,

$$\begin{aligned}
 S_{k+1} &= (1 - d - a - g_S)S_k + b_k - P_k \\
 I_{k+1} &= (1 - d - d_I - c)I_k + aS_k - T_k \\
 R_{k+1}^t &= (1 - d_R^t - g_R - h_t)R_k^t + T_k \\
 R_{k+1}^u &= (1 - d_R^u - g_R - h_u)R_k^u + cI_k \\
 H_{k+1} &= (1 - d_R - d_H)H_k + h_t R_k^t + h_u R_k^u
 \end{aligned} \tag{27}$$

where we note that the recovery rate,  $c$ , is now the untreated recovery rate. Since no population can be negative, we will enforce the constraints  $P_k \in [0, (1 - d - a - g_S)S_k + b_k]$  and  $T_k \in [0, (1 - d - d_I - c)I_k + aS_k]$  at each step by setting  $P_k, T_k$  equal to whichever bound they exceed (overriding the unconstrained optimal control derived above), which preserves the constrained optimality [10]. We now consider the different mortality rates,  $d_R^t$  and  $d_R^u$  for the treated and untreated recovered classes, as well as different rates of developing hydrocephalus,  $h_t$  and  $h_u$ . We do not have sufficient data to estimate the difference between the death rates, so we continue to set  $d_R^t = d_R^u = d_R = \frac{0047}{T_R}$ . Data pertaining to  $h_t$  and  $h_u$  is also sparse, but based on our medical experience in Uganda (SJS) we estimate that approximately 2 of every 3 sepsis cases receive treatment. Since we have estimated that 3/22.34 will develop hydrocephalus, we assume that 2/22.34 received treatment and 1/22.34 did not, so we set  $h_t = 1/22.34/T_R$  and  $h_u = 2/22.34/T_R$ .

To write the system in a compact form, we define the state variables,  $\vec{x}_k = (S_k, I_k, R_k^t, R_k^u, H_k)^\top$  and the control variables,  $\vec{u}_k = (P_k, T_k)^\top$  and we have the evolution,

$$\vec{x}_{k+1} = F\vec{x}_k + G\vec{u}_k + \vec{b}_k \quad \text{and} \quad G = \begin{pmatrix} -1 & 0 \\ 0 & -1 \\ 0 & 1 \\ 0 & 0 \\ 0 & 0 \end{pmatrix}.$$

where  $\vec{b}_k = (b, 0, 0, 0, 0)^\top$  and

$$A = \begin{pmatrix} 1 - d - a - g_S & 0 & 0 & 0 & 0 \\ a & 1 - d - d_I - c & 0 & 0 & 0 \\ 0 & 0 & 1 - d_R^t - h_t - g_R & 0 & 0 \\ 0 & c & 0 & 1 - d_R^u - h_u - g_R & 0 \\ 0 & 0 & h_t & h_u & 1 - d_R - d_H \end{pmatrix}.$$

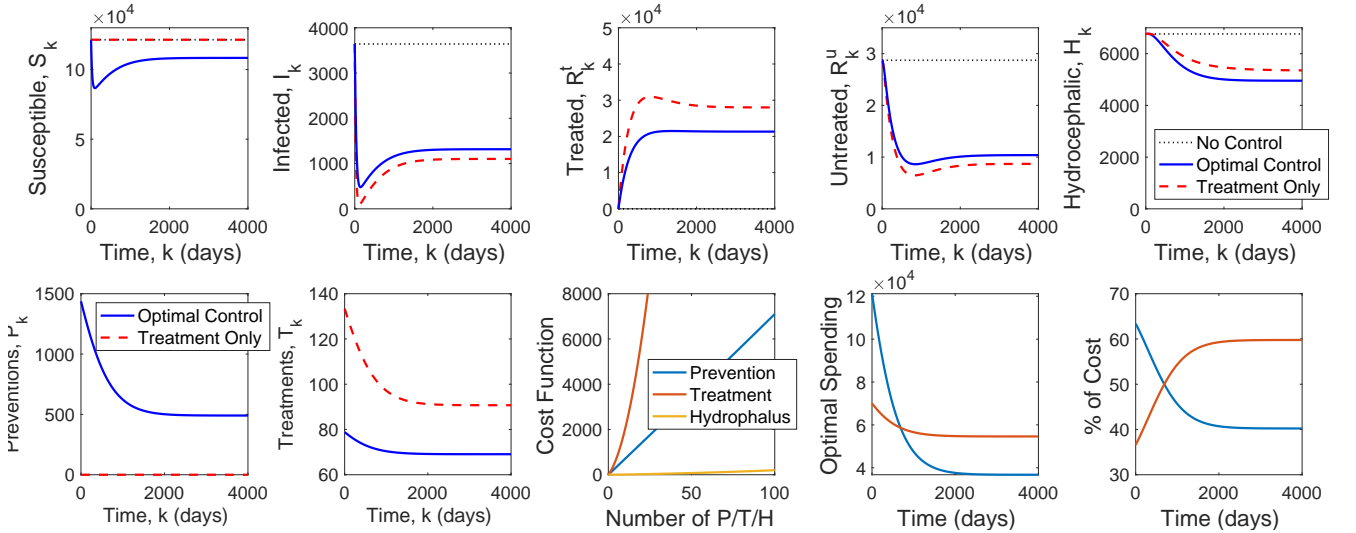


FIG. 6: Top: Starting from the uncontrolled equilibrium (black, dashed) we apply the optimal control (blue, solid) and compare to a treatment only strategy (red, dashed) using the same amount of total spending. Bottom: We show the number of effective preventions and treatments applied at each time step, the cost functions for prevention, treatment, and hydrocephalus and the actual spending of the optimal strategy.

Next, we define the cost function which balances the costs of prevention and treatment with hydrocephalus. We will only penalize cases of hydrocephalus in this study, setting  $Q = \text{diag}((0, 0, 0, 0, Q_H)^\top)$  and  $\vec{q} = (0, 0, 0, 0, q_H)^\top$ . The choice of  $Q_H, q_H$  will implicitly place a monetary cost on hydrocephalus, which has been explicitly studied [22]. Of course, one should also penalize the cost of sepsis cases [13], or possibly even deaths in each class, however balancing these terms is a complex moral and economic issue which is beyond the scope of this study. For now we consider two scenarios which exhibit the effect of this implicit cost on the optimal strategy.

Since we have two controls, prevention and treatment, we set  $R = \text{diag}((R_P, R_T)^\top)$  and  $\vec{r} = (r_P, r_T)^\top$  so altogether the cost functional is

$$J(x, u) = \sum_{k=1}^{\infty} Q_H H_k^2 + q_H H_k + R_P P_k^2 + r_P P_k + R_T T_k^2 + r_T T_k$$

(since we choose the infinite time horizon problem). For a synthetic example, we choose  $R_P = 1/100, R_T = 10$  so that treatment is more highly nonlinear than prevention and  $r_P = 70$  and  $r_T = 100$  so that prevention is less expensive than treatment. We set  $Q_H = 1/100$  to give a small penalty to non-equal distribution of cases and  $q_H = 1$ . The resulting optimal control strategy is illustrated in Fig. 6. Notice that the strategy begins with prevention to reduce the number of sepsis cases, but ultimately there are not sufficient resources to control hydrocephalus and the strategy reverts to mostly treatment as it moves to the new equilibrium. To show the advantage of the optimal strategy we compared to another strategy that spent the same amount as the optimal strategy at each time step but spent that amount purely on treatment.

Finally, to see the effect of the cost of hydrocephalus on the optimal strategy, we consider an alternative cost with  $Q_H = 1/10$  and  $q_H = 3$ . The resulting optimal strategy (and treatment only strategy) are shown in Fig. 7. Notice that the increased cost justifies a strategy that is ultimately centered around prevention, which is able to reduce hydrocephalus by nearly 80%. However, notice also that the optimal strategy to reach this end also includes a period of heavy treatment early in the simulation (the plots are shown in a logarithmic time scale to more clearly show the multiple time scales). Finally, notice that in this scenario the treatment only strategy with the same budget can only reduce hydrocephalus by 20%.

## VI. FUTURE DIRECTIONS AND CONCLUSION

In this work, we created a dynamical framework to model the interdependence of NS and PIH which cause a huge toll on human life in the developing world. The lack of communicability in these diseases enables us to utilize linear dynamics. Nevertheless, the customary Kalman filter is not well suited to assimilate such case occurrences and

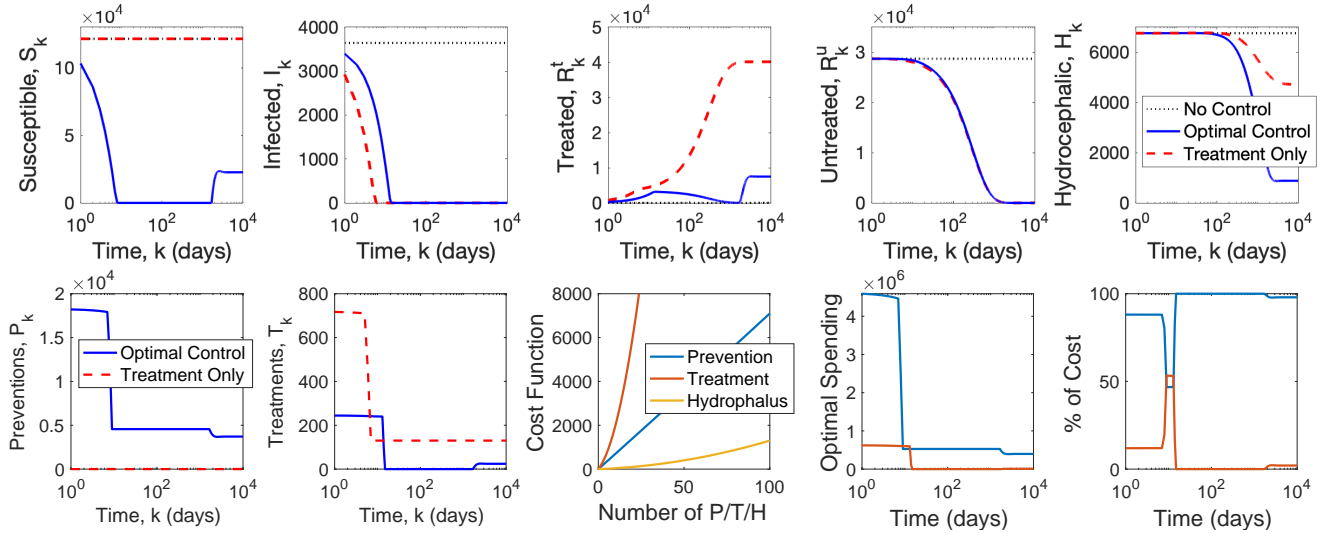


FIG. 7: Same as Figure 6 except the cost of hydrocephalus was increased by a factor of 3 with a stronger quadratic term. Shown on a logarithmic time scale so each phase of control is clearly visible. Notice that the higher cost of hydrocephalus shifts the long term strategy from mostly treatment to almost all prevention.

estimate the true number of underlying cases, or their control, because of the Poisson dynamics of case presentation. We therefore proved a novel form of Poisson Kalman Filter or PKF that is an optimal filter for such surveillance. We demonstrate the utility of this PKF, along with a general mixed linear and nonlinear cost function, to represent optimal control through treatment and prevention in this syndrome.

The mathematical methods of filtering and control had its origin with linear models, Gaussian noise, and quadratic costs. However, these assumption may not be appropriate in the context of disease modeling. Our PKF is a very general filter suitable for a broad range of non-communicable disease observations where the nonlinear interaction of susceptible and diseased individuals is not an inherent component of disease initiation. NS tends to be derived from maternal and environmental sources, but not commonly from the interaction of infants with other infants or non-maternal adults. The above results, again in the linear context, provide the foundational results from which to develop a theory appropriate to the disease context. Moreover, these solutions motivate the nonlinear methods that will extend them.

The next steps are to follow the standard approaches of the Extended Kalman Filter (EKF) and Ensemble Kalman Filter (EnKF) to generalize the Poisson Kalman Filter (PKF) to nonlinear models and observation functions. This would allow applications to contagious disease models, where control methods have been developed extensively (typically restricted to quadratic costs) [4, 19, 25–27]. Many of these methods could also be generalized to mixed linear and quadratic costs, in a manner similar to this present work. In fact, mixed linear and quadratic functions are often a better model for marginal costs, which enables the total costs to represent a cubic process.

Additionally, our case study of sepsis and hydrocephalus suggests many promising directions for future development. If a more careful tracking of cases is desired, the neonatal and infancy periods can be segmented in to multiple stages. For example, it is well known that the infections that are acquired perinatally from the mother, so called early onset sepsis, are manifest within the days of the first week of life. Infections during the subsequent weeks of the neonatal period (first 4 weeks) are environmentally acquired and are typically a very different spectrum of organisms. Therefore  $S^{(0i)}$  could represent susceptible at  $(0-i)$ -days after birth, and  $S^{(ij)}$  could represent susceptibles from  $(i-j)$ -days after birth, with varying rates and risks from sepsis at different stages of development. Another critical factor in sepsis and hydrocephalus cases is environmental variables [16], which suggests that a full spatiotemporal model will be necessary to more fully represent these dynamics. Recent findings [12] suggest the possibility of mixtures of infections in some of these infants – perhaps even a mixture of non-communicable bacteria and communicable viruses – implying a mixed linear and nonlinear model may be required to represent such co-infections. A spatiotemporal model would allow the optimal control to consider multiple methods of control and determine ideal locations and times to apply each. Finally, there is an extensive literature on the economic burdens of disease, and merging these costs with real data in settings such as we have shown has the potential to guide future policy and optimize available resources to improve public health.

## VII. ACKNOWLEDGEMENTS

We are grateful to D. Simon, M. Ferrari and M. Norton for their helpful discussions. Funded by an NIH Director's Transformative Award 1R01AI145057.

- 
- [1] Richard Bellman. *Dynamic programming*. Princeton University Press, Princeton,, 1957.
- [2] L. J. Curtis. Simple formula for the distortions in a gaussian representation of a poisson distribution. *American Journal of Physics*, 43(12):1101–1103, 1975.
- [3] M. C. Dewan, A. Rattani, R. Mekary, L. J. Glancz, I. Yunusa, R. E. Baticulon, G. Fieggen, 3rd Wellons, J. C., K. B. Park, and B. C. Warf. Global hydrocephalus epidemiology and incidence: systematic review and meta-analysis. *J Neurosurg*, pages 1–15, 2018.
- [4] Paolo Di Giamberardino and Daniela Iacoviello. A linear quadratic regulator for nonlinear sirc epidemic model. In *2019 23rd International Conference on System Theory, Control and Computing (ICSTCC)*, pages 733–738. IEEE, 2019.
- [5] Peter Diggle. *Model-based geostatistics for global public health : methods and applications*. Taylor & Francis, Boca Raton, 2019.
- [6] R. E. Kalman. A New Approach to Linear Filtering and Prediction Problems. *Journal of Basic Engineering*, 82(1):35–45, 03 1960.
- [7] M. J. Keeling and P. Rohani. *Modeling Infectious Diseases in Humans and Animals*. Princeton, Princeton, 2008.
- [8] A. V. Kulkarni, S. J. Schiff, E. Mbabazi-Kabachelor, J. Mugamba, P. Ssenyonga, R. Donnelly, J. Levenbach, V. Monga, M. Peterson, M. MacDonald, V. Cherukuri, and B. C. Warf. Endoscopic treatment versus shunting for infant hydrocephalus in uganda. *N Engl J Med*, 377(25):2456–2464, 2017.
- [9] Harold J Kushner. Stochastic stability and control. Technical report, BROWN UNIV PROVIDENCE RI, 1967.
- [10] Suzanne Lenhart and John T Workman. *Optimal control applied to biological models*. CRC press, 2007.
- [11] Jonathan H. Manton, Vikram Krishnamurthy, and Robert J. Elliott. Discrete time filters for doubly stochastic poisson processes and other exponential noise models. *Int. J. Adapt. Control Signal Process.*, 13(5):393416, August 1999.
- [12] J. N. Paulson. The bacterial and viral complexity of postinfectious hydrocephalus in uganda. *Submitted*, XX:XX–XX, 2020.
- [13] Sylvia L Ranjeva, Benjamin C Warf, and Steven J Schiff. Economic burden of neonatal sepsis in sub-saharan africa. *BMJ global health*, 3(1):e000347, 2018.
- [14] Samir K. Saha, Stephanie J. Schrag, Shams El Arifeen, Luke C. Mullany, Mohammad Shahidul Islam, Nong Shang, Shamim A. Qazi, Anita K. M. Zaidi, Zulfiqar A. Bhutta, Anuradha Bose, Pinaki Panigrahi, Sajid B. Soofi, Nicholas E. Connor, Dipak K. Mitra, Rita Isaac, Jonas M. Winchell, Melissa L. Arvay, Maksuda Islam, Yasir Shafiq, Imran Nisar, Benazir Baloch, Furqan Kabir, Murtaza Ali, Maureen H. Diaz, Radhanath Satpathy, Pritish Nanda, Bijaya K. Padhi, Sailajanandan Parida, Aneeta Hotwani, M. Hasanuzzaman, Sheraz Ahmed, Mohammad Belal Hossain, Shabina Ariff, Imran Ahmed, Syed Mamun Ibne Moin, Arif Mahmud, Jessica L. Waller, Iftekhar Rafiqullah, Mohammad A. Quaiyum, Nazma Begum, Veeraraghavan Balaji, Jasmin Halen, A. S. M. Nawshad Uddin Ahmed, Martin W. Weber, Davidson H. Hamer, Patricia L. Hibberd, Qazi Sadeq-ur Rahman, Venkat Raghava Mogan, Tanvir Hossain, Lesley McGee, Shalini Anandan, Anran Liu, Kalpana Panigrahi, Asha Mary Abraham, and Abdullah H. Baqui. Causes and incidence of community-acquired serious infections among young children in south asia (anisa): an observational cohort study. *The Lancet*, 392(10142):145–159, 2018.
- [15] S. J. Schiff. *Neural Control Engineering: The Emerging Intersection Between Control Theory and Neuroscience*. Computational neuroscience. MIT Press, 2012.
- [16] Steven J. Schiff, Sylvia L. Ranjeva, Timothy D. Sauer, and Benjamin C. Warf. Rainfall drives hydrocephalus in east africa. *Journal of neurosurgery Pediatrics*, 10(3):161–167, 2012.
- [17] Anna C. Seale, Hannah Blencowe, Alexander A. Manu, Harish Nair, Rajiv Bahl, Shamim A. Qazi, Anita K. Zaidi, James A. Berkley, Simon N. Cousens, and Joy E. Lawn. Estimates of possible severe bacterial infection in neonates in sub-saharan africa, south asia, and latin america for 2012: a systematic review and meta-analysis. *The Lancet Infectious Diseases*, 14(8):731–741, 2014.
- [18] Anna C. Seale, Hannah Blencowe, Anita Zaidi, Hammad Ganatra, Sana Syed, Cyril Engmann, Charles R. Newton, Stefania Vergnano, Barbara J. Stoll, Simon N. Cousens, and Joy E. Lawn. Neonatal severe bacterial infection impairment estimates in south asia, sub-saharan africa, and latin america for 2010. *Pediatric research*, 74:73–85, 2013.
- [19] Oluwaseun Sharomi and Tufail Malik. Optimal control in epidemiology. *Annals of Operations Research*, 251:55–71, 2017.
- [20] Dan Simon. *Optimal state estimation: Kalman, H infinity, and nonlinear approaches*. John Wiley & Sons, 2006.
- [21] UNICEF. Maternal and newborn health disparities. 2016.
- [22] Benjamin C Warf, Blake C Alkire, Salman Bhai, Christopher Hughes, Steven J Schiff, Jeffrey R Vincent, and John G Meara. Costs and benefits of neurosurgical intervention for infant hydrocephalus in sub-saharan africa: Clinical article. *Journal of Neurosurgery: Pediatrics*, 8(5):509–521, 2011.
- [23] Benjamin C. Warf, Ariella R. Dagi, Brian Nsubuga Kaaya, and Steven J. Schiff. Five-year survival and outcome of treatment for postinfectious hydrocephalus in ugandan infants. *Journal of Neurosurgery: Pediatrics PED*, 8(5):502 – 508, 2011.

- [24] Wan Yang, Alicia Karspeck, and Jeffrey Shaman. Comparison of filtering methods for the modeling and retrospective forecasting of influenza epidemics. *PLoS computational biology*, 10(4), 2014.
- [25] Tunde Tajudeen Yusuf and Francis Benyah. Optimal control of vaccination and treatment for an sir epidemiological model. *World journal of modelling and simulation*, 8(3):194–204, 2012.
- [26] Gul Zaman, Yong Han Kang, and Il Hyo Jung. Optimal vaccination and treatment in the sir epidemic model. *Proc. KSIAM*, 3:31–33, 2007.
- [27] Gul Zaman, Yong Han Kang, and Il Hyo Jung. Stability analysis and optimal vaccination of an sir epidemic model. *BioSystems*, 93(3):240–249, 2008.
- [28] Ben Zelnwirth. A generalization of the kalman filter for models with state-dependent observation variance. *Journal of the American Statistical Association*, 83(401):164–167, 1988.

## Appendix A: Optimal Linear Filter Derivation

We develop a recursive weighted least square (WLS) estimator by determining how to estimate a constant on the basis of several measurements that follow a Poisson distribution. We then use it as a basis for developing a discrete-time Kalman filter that uses Poisson distributed measurements, which we accomplish by adapting the techniques used in developing a discrete-time Kalman filter [20]. We will leave off the arrow symbols from vectors in this section to reduce the number of symbols in formulas.

### 1. Recursive weighted least squares estimator with Poisson observations

The measurement equation of a linear stochastic discrete-time dynamic system with indirect measurements of the state is given as

$$\begin{aligned} x_k &= x_{k-1} \\ y_k &= z_k, \quad z_k \sim \text{Poisson}(\lambda_k = Bx_k) \end{aligned} \quad (\text{A1})$$

where  $x_k \in \mathbb{R}^n$ ,  $y_k \in \mathbb{R}^m$  are the state vector and measurement vector respectively, and  $B \in \mathbb{R}^{m \times n}$  is a known deterministic matrix. The measurement variable  $z_k \in \mathbb{R}^m$  follows a random Poisson distribution

$$p(z_k|x_k) = \frac{(Bx_k)^{z_k}}{z_k!} e^{-(Bx_k)}, \quad z = 0, 1, 2, \dots \quad (\text{A2})$$

where the rate  $\lambda_k = Bx_k \geq 0$ . We note that the positive real rate  $\lambda_k$  equals the expected value  $E(z_k)$  and variance  $Var(z_k)$  such that

$$E(z_k) = Var(z_k) = \lambda_k$$

In our case, we assume that the state  $x$  is non-negative. We also assume that each Poisson random variable  $(z_k)_i$  has a rate that is only dependent on the corresponding state  $(x_k)_i$ , such that  $E[(z_k)_i] = c_i(x_k)_i$  where  $c_i \in \mathbb{R}_+$  are known deterministic parameters. A linear recursive estimator can be written as

$$y_k = z_k \quad (\text{A3})$$

$$\hat{x}_k = \hat{x}_{k-1} + K_k (y_k - B\hat{x}_{k-1}) \quad (\text{A4})$$

where  $K_k$  is the optimal gain matrix to be determined.

**Theorem A.1.** *The estimator of (A4) is an unbiased estimator of  $x_k$ ; that is,  $E(x - \hat{x}_k) = 0$*

*Proof.* Calculating the estimation error mean, we write

$$\begin{aligned} E(\epsilon_{x,k}) &= E(x - \hat{x}_k) \\ &= E[x - \hat{x}_{k-1} - K_k (y_k - B\hat{x}_{k-1})] \\ &= E[\epsilon_{x,k-1} - K_k (z_k - B\hat{x}_{k-1})] \\ &= E[\epsilon_{x,k-1} - K_k (z_k - Bx + Bx - B\hat{x}_{k-1})] \\ &= E[\epsilon_{x,k-1} - K_k B\epsilon_{x,k-1} - K_k (z_k - Bx)] \\ &= E[(I - K_k B)\epsilon_{x,k-1} - K_k (z_k - Bx)] \\ &= (I - K_k B) E(\epsilon_{x,k-1}) - K_k (E(z_k) - Bx) \end{aligned} \quad (\text{A5})$$

So if  $E(z_k) = Bx$  and  $E(\epsilon_{x,k-1}) = 0$ , then  $E(\epsilon_{x,k}) = 0$ . Therefore (A4) is an unbiased estimator. This property holds regardless of the value of the gain matrix  $K_k$ . This implies that, on average, the state estimate  $\hat{x}$  will be equal to the true state  $x$ , when measurements – that follow a Poisson distribution whose rate is dependent on the state – are taken.  $\square$

**Theorem A.2.** *Among all linear filters, the filter given by the linear estimator of A4 with gain matrix  $K_k$  given by*

$$K_k = P_{k-1}B^T (BP_{k-1}B^T + V_k)^{-1}$$

*is optimal in the sense of minimal sum of squared errors when  $V_k = \text{diag}(Bx_k)$ . In other words,*

$$\frac{\partial J_k}{\partial K_k} = 0$$

where

$$J_k = \text{trace}(P_k) = \mathbb{E}[|\hat{x}_k - \bar{x}_k|_2^2] = \sum_i \mathbb{E}[(\hat{x}_k - \bar{x}_k)_i^2]$$

*Proof.* Using (A5), we solve for the estimation error covariance  $P_k$  as

$$\begin{aligned} P_k &= E[\epsilon_{x,k}\epsilon_{x,k}^T] \\ &= E\left\{[(I - K_k B)\epsilon_{x,k-1} - K_k(z_k - Bx)] [\epsilon_{x,k-1}^T(I - K_k B)^T - (z_k - Bx)^T K_k^T]^T\right\} \\ &= (I - K_k B)E[\epsilon_{x,k-1}\epsilon_{x,k-1}^T](I - K_k B)^T - (I - K_k B)E[\epsilon_{x,k-1}(z_k - Bx)^T]K_k^T \\ &\quad - K_k E[(z_k - Bx)\epsilon_{x,k-1}^T](I - K_k B)^T + K_k E[(z_k - Bx)(z_k - Bx)^T]K_k^T \end{aligned} \quad (\text{A6})$$

Since the estimation error at time  $k-1$  given by  $\epsilon_{x,k-1} = x - \hat{x}_{k-1}$  is independent of the measurement  $z_k$  at time  $k$ , we have

$$\begin{aligned} E[\epsilon_{x,k-1}(z_k - Bx)^T] &= E[\epsilon_{x,k-1}]E[(z_k - Bx)^T] \\ &= 0 \end{aligned}$$

since the expected value  $E(\epsilon_{x,k-1})$  and  $E(z_k - Bx)$  are both zero. More generally, when  $x$  is a random variable,  $\epsilon_{x,k-1}$  may not be independent of the measurement  $z_k$ , however, the above expectation is still zero since,

$$\begin{aligned} E[\epsilon_{x,k-1}(z_k - Bx)^T] &= E[(x - \hat{x}_{k-1})(z_k - Bx)^T] \\ &= E[E[(x - \hat{x}_{k-1})(z_k - Bx)^T | x]] \\ &= E[(x - \hat{x}_{k-1})E[(z_k - Bx)^T | x]] \\ &= E[(x - \hat{x}_{k-1})(E[z_k | x] - Bx)^T] \\ &= E[(x - \hat{x}_{k-1})(Bx - Bx)^T] \\ &= 0 \end{aligned}$$

by the law of total expectation. Therefore, (A6) reduces to

$$P_k = (I - K_k B)E[\epsilon_{x,k-1}\epsilon_{x,k-1}^T](I - K_k B)^T + K_k E[(z_k - Bx)(z_k - Bx)^T]K_k^T \quad (\text{A7})$$

Using the fact that  $Bx = E[z_k]$ , we rewrite (A7) as

$$P_k = (I - K_k B)E[\epsilon_{x,k-1}\epsilon_{x,k-1}^T](I - K_k B)^T + K_k E[(z_k - E[z_k])(z_k - E[z_k])^T]K_k^T \quad (\text{A8})$$

Recall that for a random variable  $Y$  with mean  $E[Y]$ , the  $i$ th central moment of  $Y$ , which is written as

$$i\text{th central moment of } Y = E[(Y - E[Y])^i]$$

equals its variance when  $i = 2$  (see Chapter 2 of [20]). Therefore,

$$E[(z_k - E[z_k])(z_k - E[z_k])^T] = V_k \quad (\text{A9})$$

where  $V_k \in \mathbb{R}^{m \times m}$ , which is written as  $V_k = \text{diag}(Bx_k)$ , is the covariance of  $z_k$ . Substituting (A9) into (A8) gives

$$P_k = (I - K_k B)P_{k-1}(I - K_k B)^T + K_k V_k K_k^T \quad (\text{A10})$$

which is the recursive formula for determining the covariance of the least squares estimation error. We then minimize the sum of the estimation error variances at time  $k$ . From the cost function

$$J_k = \text{trace}(P_k) \quad (\text{A11})$$

we write

$$\frac{\partial J_k}{\partial K_k} = 2(I - K_k B)P_{k-1}(-B)^T + 2K_k V_k \quad (\text{A12})$$

Setting (A12) equal to zero to find the value of  $K_k$  that minimizes  $J_k$ ,

$$\begin{aligned} K_k V_k &= (I - K_k B)P_{k-1}B^T \\ K_k (V_k + B P_{k-1} B^T) &= P_{k-1} B^T \\ K_k &= P_{k-1} B^T (B P_{k-1} B^T + V_k)^{-1} \end{aligned} \quad (\text{A13})$$

This implies that the optimal gain matrix  $K_k$  given by (A13) minimizes the sum of squared errors when  $V_k = \text{diag}(Bx_k)$ . □

We note that if all the states  $x$  are used to generate the output  $y$ , such that each state  $x_i$  is used to generate its Poisson random measurement  $z_i$ , then  $V_k = \text{diag}([c_1 x_{1k}, c_2 x_{2k}, \dots, c_m x_{mk}])$  where  $m = n$ . Since the true state  $x_k$  is unavailable to the estimator, we replace  $x_k$  with  $\hat{x}_{k-1}$ . Therefore we have

$$V_k = \text{diag}([c_1 \hat{x}_{1k-1}, c_2 \hat{x}_{2k-1}, \dots, c_m \hat{x}_{mk-1}]) = \text{diag}(B\hat{x}_{k-1})$$

which results in a suboptimal filter.

### Recursive weighted least square estimator algorithm

#### 1 Initialization

$$\begin{aligned} \hat{x}_0 &= E(x) \\ P_0 &= E[(x - \hat{x}_0)(x - \hat{x}_0)^T] \end{aligned}$$

#### 2 Estimation

$$K_k = P_{k-1} B^T (B P_{k-1} B^T + V_k)^{-1} \quad (\text{A14})$$

$$\hat{x}_k = \hat{x}_{k-1} + K_k (y_k - B\hat{x}_{k-1}) \quad (\text{A15})$$

$$P_k = (I - K_k B)P_{k-1}(I - K_k B)^T + K_k V_k K_k^T \quad (\text{A16})$$

## 2. Kalman filter based on WLS with Poisson observations

Consider the linear stochastic discrete-time dynamic system with indirect measurements of the state given by

$$x_k = F_{k-1}x_{k-1} + G_{k-1}u_{k-1} + w_{k-1}, \quad w_k \sim \mathcal{N}(0, \sigma^2) \quad (\text{A17})$$

$$y_k = z_k, \quad z_k \sim \text{Poisson}(\lambda_k = Bx_k) \quad (\text{A18})$$

The expected value of both sides of (A17) is given as

$$\bar{x}_k = E(x_k) = F_{k-1}\bar{x}_{k-1} + G_{k-1}u_{k-1} \quad (\text{A19})$$

Using

$$(x_k - \bar{x}_k)(x_k - \bar{x}_k)^T = F_{k-1}(x_{k-1} - \bar{x}_{k-1})(x_{k-1} - \bar{x}_{k-1})^T F_{k-1}^T + w_{k-1}w_{k-1}^T + F_{k-1}(x_{k-1} - \bar{x}_{k-1})w_{k-1}^T + w_{k-1}(x_{k-1} - \bar{x}_{k-1})^T F_{k-1}^T \quad (\text{A20})$$

the covariance of  $x_k$  is given as

$$P_k^- = E[(x_k - \bar{x}_k)(x_k - \bar{x}_k)^T] = F_{k-1}P_{k-1}^+ F_{k-1}^T + W_{k-1} \quad (\text{A21})$$

because  $E[(x_{k-1} - \bar{x}_{k-1})w_{k-1}^T] = 0$ , since  $(x_{k-1} - \bar{x}_{k-1})$  is uncorrelated with  $w_{k-1}$ . Therefore from (A21), (A14), (A15), and (A16), we replace  $\hat{x}_{k-1}$  with  $\hat{x}_k^-$ , we replace  $P_{k-1}$  with  $P_k^-$ , we replace  $\hat{x}_k$  with  $\hat{x}_k^+$ , and we replace  $P_k$  with  $P_k^+$ . We then get the Poisson Kalman filter equations for each time step  $k = 1, 2, \dots$ :

$$\hat{x}_k^+ = \hat{x}_k^- + K_k (y_k - B\hat{x}_k^-) \quad (\text{A22})$$

$$P_k^- = F_{k-1}P_{k-1}^+ F_{k-1}^T + W_{k-1} \quad (\text{A23})$$

$$K_k = P_k^- B^T (B P_k^- B^T + V_k)^{-1} \quad (\text{A24})$$

$$\hat{x}_k^- = F_{k-1}\hat{x}_{k-1}^+ + G_{k-1}u_{k-1} \quad (\text{A25})$$

$$P_k^+ = (I - K_k B)P_k^- (I - K_k B)^T + K_k V_k K_k^T \quad (\text{A26})$$

## Appendix B: Optimal control with mixed quadratic and linear cost

As in A, we will leave off the arrow symbols from vectors in this section to reduce the number of symbols in formulas. To derive LQ equations with forcing and linear terms in the cost function we consider the evolution

$$x_{k+1} = Fx_k + Gu_k + b_k$$

where  $b_k$  is a non-autonomous input. We consider the cost functional

$$J(x, u) = \sum_{k=1}^T \frac{1}{2} x_k^\top Q x_k + x_k^\top q + \frac{1}{2} u_k^\top R u_k + u_k^\top r$$

which has linear terms defined by the vectors  $q, r$ . Plugging into the Bellman equation [1],

$$M_k(x_k) = \frac{1}{2} x_k^\top Q x_k + x_k^\top q + \min_{u_k} \left\{ \frac{1}{2} u_k^\top R u_k + u_k^\top r + M_{k+1}(Fx_k + Gu_k + b_k) \right\}$$

and assuming  $M_k(x_k) = \frac{1}{2} x_k^\top P_k x_k + p_k^\top x_k + d_k$  and  $M_{k+1}(x) = \frac{1}{2} x^\top P_{k+1} x + p_{k+1}^\top x + d_{k+1}$  we have

$$\begin{aligned} & x_k^\top P_k x_k + p_k^\top x_k + d_k \quad (\text{B1}) \\ &= \frac{1}{2} x_k^\top Q x_k + x_k^\top q + d_{k+1} \\ &+ \min_{u_k} \left\{ \frac{1}{2} u_k^\top R u_k + u_k^\top r + \frac{1}{2} (Fx_k + Gu_k + b_k)^\top P_{k+1} (Fx_k + Gu_k + b_k) + p_{k+1}^\top (Fx_k + Gu_k + b_k) \right\} \\ &= \frac{1}{2} x_k^\top (Q + F^\top P_{k+1} F) x_k + x_k^\top (q + F^\top p_{k+1} + F^\top P_{k+1} b_k) + d_{k+1} + b_k^\top \left( p_{k+1} + \frac{1}{2} P_{k+1} b_k \right) \\ &+ \min_{u_k} \left\{ \frac{1}{2} u_k^\top (R + G^\top P_{k+1} G) u_k + u_k^\top (r + G^\top p_{k+1} + G^\top P_{k+1} (Fx_k + b_k)) \right\} \end{aligned}$$

taking the derivative with respect to  $u_k$  to minimize we find

$$u_k^\top R + r^\top + (Fx_k + Gu_k + b_k)^\top P_{k+1} G + p_{k+1}^\top G = 0$$

so the minimum is achieved with control

$$u_k = -(R + G^\top P_{k+1} G)^{-1} (G^\top (P_{k+1} (Fx_k + b_k) + p_{k+1}) + r) \quad (\text{B2})$$

and plugging this control in (B1) we find

$$\begin{aligned}
& x_k^\top P_k x_k + p_k^\top x_k + d_k \tag{B3} \\
&= \frac{1}{2} x_k^\top (Q + F^\top P_{k+1} F) x_k + x_k^\top (q + F^\top p_{k+1} + F^\top P_{k+1} b_k) + d_{k+1} + b_k^\top \left( p_{k+1} + \frac{1}{2} P_{k+1} b_k \right) \\
&\quad - \frac{1}{2} ((x_k^\top F^\top + b_k^\top) P_{k+1} + p_{k+1}^\top) G + r^\top (R + G^\top P_{k+1} G)^{-1} (G^\top (P_{k+1} (F x_k + b_k) + p_{k+1}) + r) \\
&= \frac{1}{2} x_k^\top (Q + F^\top P_{k+1} F - F^\top P_{k+1} G (R + G^\top P_{k+1} G)^{-1} G^\top P_{k+1} F) x_k \\
&\quad + x_k^\top (q + F^\top p_{k+1} + F^\top P_{k+1} b_k - F^\top P_{k+1} G (R + G^\top P_{k+1} G)^{-1} (G^\top (P_{k+1} b_k + p_{k+1}) + r)) \\
&\quad + \frac{1}{2} ((b_k^\top P_{k+1} + p_{k+1}^\top) G + r^\top) (R + G^\top P_{k+1} G)^{-1} (G^\top (P_{k+1} b_k + p_{k+1}) + r) \\
&\quad + d_{k+1} + b_k^\top \left( p_{k+1} + \frac{1}{2} P_{k+1} b_k \right).
\end{aligned}$$

Since the constant term  $d_k$  does not appear in the optimal control, we only need to solve for  $P_k$  and  $p_k$  by matching quadratic and linear coefficients of the left and right sides of the above equation. The quadratic term gives the expected discrete Riccati equation

$$P_k = F^\top P_{k+1} F - F^\top P_{k+1} G (R + G^\top P_{k+1} G)^{-1} G^\top P_{k+1} F + Q$$

and the linear term determines  $p_k$  by

$$p_k = F^\top (P_{k+1} b_k + p_{k+1}) - F^\top P_{k+1} G (R + G^\top P_{k+1} G)^{-1} (G^\top (P_{k+1} b_k + p_{k+1}) + r) + q$$

then  $P_k$  and  $p_k$  determine the optimal control (B2).

For infinite time horizon we obtain the algebraic Riccati equation

$$P_\infty = F^\top P_\infty F - F^\top P_\infty G (R + G^\top P_\infty G)^{-1} G^\top P_\infty F + Q$$

and with constant forcing  $b_k = b$  we find

$$p_\infty = (I - F^\top + F^\top P_\infty G (R + G^\top P_\infty G)^{-1} G^\top)^{-1} (F^\top P_\infty b - F^\top P_\infty G (R + G^\top P_\infty G)^{-1} (G^\top P_\infty b + r) + q)$$

and if  $r = q = 0$  this reduces to

$$p_\infty = \left( (F^\top - F^\top P_\infty G (R + G^\top P_\infty G)^{-1} G^\top)^{-1} - I \right)^{-1} P_\infty b$$

and

$$u_\infty = -(R + G^\top P_\infty G)^{-1} G^\top (P_\infty (F x_k + c) + p_\infty)$$

which is the optimal control for the system with forcing  $b$  and a purely quadratic cost.